NUMERICAL APPROXIMATION OF BLOW-UP OF RADIALLY SYMMETRIC SOLUTIONS OF THE NONLINEAR SCHRÖDINGER EQUATION

G. D. AKRIVIS, V. A. DOUGALIS, O. A. KARAKASHIAN, AND W. R. MCKINNEY

ABSTRACT. We consider the initial-value problem for the radially symmetric nonlinear Schrödinger equation with cubic nonlinearity (NLS) in $d = 2$ and 3 space dimensions. To approximate smooth solutions of this problem, we construct and analyze a numerical method based on a standard Galerkin finite element spatial discretization with piecewise linear, continuous functions and on an implicit Crank–Nicolson type time-stepping procedure. We then equip this scheme with an adaptive spatial and temporal mesh refinement mechanism that enables the numerical technique to approximate well singular solutions of the NLS that blow up at the origin as the temporal variable t tends from below to a finite value $t^\star$. For the blow-up of the amplitude of the solution we recover numerically the well-known rate $(t^\star - t)^{-\frac{1}{2}}$ for $d = 3$. For $d = 2$ our numerical evidence supports the validity of the 'log log' law $[\ln \ln \frac{1}{t^\star - t}/(t^\star - t)]^{1/2}$ for t extremely close to $t^\star$. The scheme also approximates well the details of the blow-up of the phase of the solution at the origin as $t \to t^\star$.

1. INTRODUCTION

The nonlinear Schrödinger equation with cubic nonlinearity (henceforth referred to as "NLS equation") is given by

$$u_t = \mathrm{i}\Delta u + \mathrm{i}|u|^2 u, \quad x \in \mathbb{R}^d, \quad t \geq 0, \tag{1.1a}$$

wherein u is a complex-valued function of the 'spatial' variable $x \in \mathbb{R}^d$, $d = 1, 2, 3$, and of the 'temporal' variable $t \geq 0$. The equation occurs frequently in various areas of Mathematical Physics, posed as an initial-value problem with given initial condition

$$u(x, 0) = u^0(x), \quad x \in \mathbb{R}^d. \tag{1.1b}$$

For example, for $d = 1$ it arises as an envelope equation in water wave theory, [53]. In two space dimensions it occurs in nonlinear optics, where it describes in certain regimes the propagation of electromagnetic beams in media whose index of refraction depends on the amplitude of the field in a simple nonlinear way, [14], [44]. For $d = 3$ it is obtained as a limiting case of Zakharov's model of Langmuir waves, [51]. We refer the reader to the surveys [52], [36], [37], and, especially, to the recent monograph [42] for discussions of various issues regarding the physical background, the derivation and validity of NLS.

It is not hard to see that for $d = 1$ the initial-value problem (1.1a–b) is globally well-posed for smooth enough initial data that decays sufficiently fast at infinity. It is also well known that in this case it can be solved by the inverse scattering transform, [53]. For $d = 2, 3$ we have, in appropriate function spaces, local well–posedness, cf., e.g., [21], [26], and global well–posedness for suitably restricted initial data, [13], [49]. It is also well known that for $d \geq 2$ there exist singular solutions which blow up in L^∞ in finite time, [51], [22]. The blow-up in the critical,

2000 *Mathematics Subject Classification.* 35Q55, 65M60, 65M50.

Key words and phrases. Nonlinear Schrödinger equation, point blow-up, finite element methods, adaptive mesh refinement.

two-dimensional case is usually referred to as "self-trapping" or "self-focusing", whereas the blow-up in the supercritical, three-dimensional case is sometimes referred to as "collapse". In [40], [13], [12], [20], [35], [42] the reader will find detailed surveys and expositions of existing rigorous results on the well–posedness and on the blow–up of solutions of (1.1a–b).

In this paper we shall be interested in the numerical approximation of radially symmetric solutions of the initial-valued problem for the NLS in $d = 2$ and 3 dimensions. We make therefore the hypothesis that the function u^0 in the initial condition (1.1b) and, consequently, the solution of (1.1a) are radially symmetric, i.e., that $u = u(r,t)$ for $t \geq 0$, where $r = (x_1^2 + \cdots + x_d^2)^{\frac{1}{2}}$. Hence our problem becomes

$$u_t = \mathrm{i}(u_{rr} + \frac{d-1}{r}u_r) + \mathrm{i}|u|^2 u, \quad r > 0, \quad t \geq 0, \tag{1.2a}$$

$$u_r(0,t) = 0, \qquad t \geq 0, \tag{1.2b}$$

$$u(r,0) = u^0(r), \quad r \geq 0. \tag{1.2c}$$

It is straightforward to check that the L^2 norm and the Hamiltonian of the solution of (1.1a–b) are conserved. In the presence of radial symmetry, i.e. for problem (1.2a–c), these invariants are

$$\int_0^\infty |u(r,t)|^2 r^{d-1} dr = \text{const. for } t \geq 0, \tag{1.3}$$

$$\int_0^\infty \left(|u_r(r,t)|^2 - \frac{1}{2}|u(r,t)|^4 \right) r^{d-1} dr = \text{const. for } t \geq 0. \tag{1.4}$$

There has appeared by now a considerable amount of work aimed at describing in detail, by numerical and asymptotic means, the characteristics of the blow-up of solutions of (1.2 a–c) for $d = 3$ and 2. We refer the reader to a series of publications, [43], [34], [30], [31], [28], [32], [29], [41] of a group including Papanicolaou, C. Sulem, P.–L. Sulem and their co-workers. We also refer to the work of the group of Zakharov and his co-workers, which went on for many years and was conveniently summarized in [27]; this paper also contains references to earlier Russian work on the subject. For more recent work in the critical case cf. [33], [16], [18]; for more references and an authoritative overall exposition of this body of work, we refer the reader to [42].

As a result of this research, there is a wealth of evidence on the main characteristics of the blow-up singularity in the presence of radial symmetry for $d = 3$. The problem was studied in [34] by use of a numerical technique that employs "dynamic rescaling", a time-dependent change of scales of the solution and the independent variables of (1.2a). The scaling factors are chosen so that suitable functionals of the solution are preserved. It turns out that the transformed dependent variable satisfies a p.d.e. with global smooth solution. This equation is integrated numerically and the details of the blow-up are inferred from the long-time asymptotics of the numerical solution and the scale factors. In this manner, it was concluded in [34] that singular radial solutions in $d = 3$ dimensions evolve into a self-similar form and blow up at the origin with an amplitude peak that grows like $(t^\star - t)^{-\frac{1}{2}}$ as t approaches the blow-up time $t^\star < \infty$. The computations also provided additional information on the basis of which further conclusions were drawn in [34] on the details of the self-similar structure of the solution and the singularity of its phase as $t \uparrow t^\star$. Some of these features of the blow-up had been predicted by Zakharov [51]; see [27] for an account of the largely parallel and analogous work of the Russian school on three-dimensional collapse.

In the two-dimensional case, still for radially symmetric solutions, earlier conclusions in the literature on the blow-up rate of the amplitude, based on numerical and asymptotic computations, varied substantially. This is not surprising; $d = 2$ is the critical dimension case for the cubic nonlinearity, and the blow-up slows down somewhat, making the numerical integration of the equation harder. Thus, a $(t^\star - t)^{-2/3}$ law for the blow-up of the amplitude was conjectured in [54] and [43], while $\left[\ln \frac{1}{t^\star - t}/(t^\star - t)\right]^{\frac{1}{2}}$ was put forward in [48] and [50]. It soon became apparent that the amplitude behaved *grosso modo* like $(t^\star - t)^{-\frac{1}{2}}$ but that this behavior was perturbed by a slower varying factor. Using computational (dynamic rescaling) evidence and asymptotic techniques LeMesurier *et al.*, [30], suggested the form $\left[F(t^\star - t)/(t^\star - t)\right]^{\frac{1}{2}}$, wherein, as $s \downarrow 0$, $F(s)$ tends to infinity more slowly than $(\ln \frac{1}{s})^\gamma$ for any $\gamma > 0$. Finally, in [28] and [32] it was concluded that the rate is $[\ln \ln \frac{1}{t^\star - t}/(t^\star - t)]^{1/2}$. This rate had been predicted by Fraiman, [19], [39], on the basis of asymptotic estimates. The Zakharov group favored rates of the form $[\big(\ln \frac{1}{t^\star - t}\big)^\gamma/(t^\star - t)]^{1/2}$ for $0.35 \leq \gamma \leq 0.65$, depending on the initial conditions, [27], but estimated that the log log rate probably obtains for t extremely close to $t^\star$. The latter conclusion is still maintained in the recent papers [33], [16], [18], where new, 'adiabatic' rates are proposed; these describe accurately the blow-up in its earlier stages and agree asymptotically with the log log law.

In a recent paper Budd *et al.*, [11], have studied by numerical and analytical techniques the self-similar profile of the solution of the NLS for $d > 2$ and identified new multi-peak structures. To investigate the stability of these solutions they integrated numerically the NLS using a semidiscretization on a moving radial mesh that evolves in time, getting finer near the singularity, and takes into account scale invariance properties of the NLS.

As an alternative to change of variables and asymptotic techniques one can also approximate singular solutions of (1.2) by direct numerical integration of the p.d.e. in the r, t, u variables. In the past such direct numerical simulations for the NLS were used, e.g., in [48] (see also the references in [27]), [50], [43], [45]. As the solution blows up, its accurate approximation requires using extremely fine mesh refinement in the spatial variable around the blow-up point, and radically decreasing the time step sizes as t approaches $t^\star$. Avoiding the deterioration of the numerical results due to roundoff errors in computing the solution and various quantities of interest derived therefrom (such as blow-up rates), becomes then an overarching consideration, as pointed out by the authors of [27] in their critique of direct integration techniques.

There is a growing amount of research reported in the literature concerning the direct numerical integration of various p.d.e's, whose solutions (or some other associated quantities of interest) blow up at a point in finite time. We mention as examples the papers by Berger and Kohn [7], by Dupont *et al.* [15], and Bertozzi *et al.* [8], where adaptive grid refinement algorithms have been used to approximate the singularities of the solutions. In [7] a simple explicit finite difference method is used as a base for constructing a scheme with adaptive spatial and temporal mesh refinement mechanisms; the latter is then employed to approximate the detailed space and time structure of even solutions of the one–dimensional semilinear heat equation close to blow-up. The adaptive algorithm of [7] includes several quite interesting features including the rescaling of the solution on the finest spatial mesh interval. The extent of that interval is estimated automatically and the boundary conditions required at its endpoints are provided by an accompanying calculation with larger time steps in the coarse mesh regions. In [15] the authors study a Hele–Shaw system of two fluids (air–water) in the lubrication approximation. The mathematical model is a system of three equations in one space dimension with unknowns the pressure, the velocity and the thickness of the water layer, and is posed with data that

allow the water thickness to go to zero at some point $x^\star$ at a finite time $t^\star$ causing e.g. the gradient of the velocity to blow up. (In [8] related models of flows of thin viscous films are also considered.) The numerical study of such a problem has many similarities with a blow-up calculation: The classical solution breaks down at $t^\star$ and it is of interest to determine several quantities of the flow as functions of $t^\star - t$ when $t \uparrow t^\star$. The discretization is effected by an implicit finite difference scheme endowed with an adaptive mechanism that refines the spatial mesh around $x^\star$ and reduces the time step according to various criteria as $t \uparrow t^\star$.

Of interest in these works is not only the adaptive mesh refinement technology but also the various data fitting schemes that the authors use, with the aid of asymptotic analysis, to determine the fine structure of solutions near the singularity. In this connection one should also mention the data fitting ideas employed by Shelley (cf., e.g., [38] and its references) in describing the development of singularities in the motion of vortex sheets by solving numerically the Birkhoff integrodifferential equation on uniform meshes.

In the paper at hand we shall approximate solutions of the initial– and boundary–value problem (1.2a–b–c) for NLS for $d = 2$ and 3 that blow up at the origin. We shall use as a base scheme a fully discrete Galerkin finite element discretization with continuous piecewise linear functions on a partition of a finite interval in the radial variable, coupled with an implicit Crank–Nicolson type time–stepping procedure. In Section 2 we address issues of stability and convergence of this base scheme in the case of smooth solutions, and state without proof the relevant error estimates which are extensions to the radial case of results of [1], [23] and [2]. All our theoretical error estimates hold under the hypotheses that the solution of the p.d.e. is smooth, the spatial partition is quasiuniform and the temporal step is constant. However this will not deter us from proposing suitably adaptive versions of these methods and approximating with them solutions that blow up in finite time.

The specific spatial and temporal mesh refinement technique that we use is in a very general sense similar to the ones of [7] and [15]. It is an application to the case of NLS of the mesh refinement strategy that three of us have used in the past, in collaboration with J. Bona, to approximate the blow-up of solutions of the generalized Korteweg–de Vries equation, cf., e.g., [9], [10]. The spatial mesh refinement technique, described in detail in section 3, consists of a mechanism of reducing automatically the mesh size in the neighborhood of the origin, as the amplitude of the solution steepens, by means of a check on a local $L^\infty - L^2$ inverse inequality satisfied by members of the finite element subspace. The criterion for cutting the time step is based on controlling a suitably normalized version of the second invariant (Hamiltonian) of the problem. We found that the adaptive mechanism worked well in three as well as two dimensions, allowing numerical solutions to reach maximum values of the ratio $|u(0,t)|/|u^0(0)|$ of "final" to initial amplitude at the origin of up to $O(10^{15})$ for t extremely close to the blow-up time $t^\star$.

In section 4 we consider the three-dimensional case and report our numerical computations of rates of blow-up of the amplitude, of various norms of the solution, and of its phase as $t \to t^\star$. Paying particular attention to the numerical stability of these rate computations, we verify, using several initial profiles, the self-similar form of the blow-up and the amplitude blow-up law $(t^\star - t)^{-\frac{1}{2}}$ and reproduce accurately the value of the constant κ, cf. [34], [27], that occurs, e.g., in the formula for the singularity of the phase of the solution, i.e. in the expression $\exp\left(\mathrm{i}\kappa \ln \frac{1}{t^\star - t}\right)$ as $t \to t^\star$.

In section 5 we turn to the two-dimensional case. We test several laws for the blow-up rate of the amplitude against the results of our numerical simulations for t extremely close to $t^\star$. Our conclusion is that the log log rate of [28], [32], [19], provides a highly accurate fit to our data for t extremely close to $t^\star$. The description of the phase singularity turns out to be quite a

challenging problem in two dimensions, cf. [28]. We confirm numerically that the approximate value of the constant λ occurring e.g. in the expression of the phase of the singular solution at $r = 0$ (which, to first-order terms, is $\exp\left(\frac{1}{2\lambda}\ln\frac{1}{t^\star - t}\ln\ln\frac{1}{t^\star - t}\right)$ according to [28]) is equal to π, something that was predicted on the basis of a "descent" argument from higher dimensions in [28] but not actually seen in numerical simulations of the evolution equation in that work, and was later verified by asymptotic analysis in [41].

We close with a section of conclusions, extensions and comments on related research directions. A preliminary report of some of the results of this paper appeared in [3].

2. FULLY DISCRETE GALERKIN APPROXIMATIONS OF SMOOTH SOLUTIONS

In this section we consider the radial problem (1.2) posed on a finite interval $0 \le r \le R$ with zero Dirichlet boundary condition at $r = R$. As we will be interested eventually in describing the evolution of profiles that focus (collapse) fast at $r = 0$, the solutions on the finite spatial internal will furnish a reasonable approximation to those of (1.2), for large R and initial data u^0 that decay exponentially, say, with r. To normalize matters, we shall scale the radial variable so that it takes values between zero and one. To that effect, after scaling $r \leftarrow r/R$, we consider the problem (for $T > 0$ large enough)

$$u_t = \mathrm{i}\varepsilon(u_{rr} + \frac{d-1}{r}u_r) + \mathrm{i}|u|^2 u,\ (r,t) \in (0,1] \times [0,T], \tag{2.1a}$$

$$u_r(0,t) = 0, \qquad 0 \le t \le T, \tag{2.1b}$$

$$u(1,t) = 0, \qquad 0 \le t \le T, \tag{2.1c}$$

$$u(r,0) = v(r), \quad 0 \le r \le 1, \tag{2.1d}$$

where $d = 2$ or $3, \varepsilon = 1/R^2$, and $v(x) = u^0(xR)$, $0 \le x \le 1$. The solution of this problem satisfies analogs of (1.3) and (1.4), i.e. preserves the invariants

$$\int_0^1 |u(r,t)|^2 r^{d-1} dr = \int_0^1 |v(r)|^2 r^{d-1} dr, \tag{2.2}$$

and

$$\begin{aligned} H(u(t)) &:= \int_0^1 (\varepsilon|u_r(r,t)|^2 - \frac{1}{2}|u(r,t)|^4) r^{d-1} dr \\ &= \int_0^1 (\varepsilon|v_r(r)|^2 - \frac{1}{2}|v(r)|^4) r^{d-1} dr =: H(v), \end{aligned} \tag{2.3}$$

for $0 \le t \le T$. In the sequel, we shall denote L^p norms, $1 \le p < \infty$, of radial functions defined on $[0,1]$ by

$$\|f\|_{L^p} = \left(\int_0^1 |f(r)|^p r^{d-1} dr\right)^{\frac{1}{p}},$$

and put $\|f\| = \|f\|_{L^2}$, $\|f\|_{L^\infty} = \operatorname{ess\,sup}_{0 \le r \le 1} |f(r)|$. The L^2 inner product $\int_0^1 f(r)\overline{g(r)} r^{d-1} dr$ will be denoted by (f, g).

We shall approximate the solution of (2.1) by a simple fully discrete Galerkin–finite element method that uses continuous, piecewise linear polynomials in r and the implicit 'midpoint' time–stepping rule in t. (We could have instead lumped the elements of the mass matrix, used a simple quadrature rule for the nonlinear term, and worked equally well with the resulting finite difference scheme. However, we had a finite element code handy, having originally implemented a more general program using up to cubic splines in space and various high order implicit

Runge–Kutta schemes in time as we had previously done in the generalized KdV case. There were indeed some NLS computations in which a higher order code had certain advantages. However, for all numerical experiments reported in this paper the present second–order scheme proved quite satisfactory. Another reason for introducing finite elements is to set the stage for a new code in the 2−D, nonradial case, about which cf. Section 6.)

The stability and convergence of fully discrete finite element methods have been analyzed in detail in [1] and [23] for the NLS in Cartesian coordinates. Although there are several instances where the techniques of the convergence proofs in the radial case depart from their Cartesian counterparts, the overall theory remains basically the same. Hence, in this section we shall just establish notation and state our results without proof. Our error estimates require that the solution of (2.1) is sufficiently smooth in $[0,1]\times[0,T]$, that the radial mesh is quasiuniform and the time step is constant. However, in subsequent sections we shall use adaptive versions of our schemes to approximate singular solutions as they blow up. This will require drastic local refinement of the radial mesh and fast reduction of the temporal step to extremely small values. There is as yet no satisfactory convergence theory available for such adaptive schemes.

Let $0=r_0<r_1<\cdots<r_N=1$ be a quasiuniform partition of $[0,1]$ with $h=\max_i(r_i-r_{i-1})$. Let S_h be the space of complex-valued continuous functions on $[0,1]$ that vanish at $r=1$ and are linear polynomials on each interval (r_{i-1},r_i). The standard Galerkin semidiscretization of (2.1) on S_h is defined in the customary way as a map $u_h:[0,T]\to S_h$ satisfying the equations

$$(u_{ht},\chi)+\mathrm{i}\varepsilon(u_{hr},\chi_r)=\mathrm{i}(|u_h|^2u_h,\chi)\quad\forall\chi\in S_h,\quad 0\le t\le T, \tag{2.4a}$$

$$u_h(0)=v_h, \tag{2.4b}$$

where v_h is the L^2 projection of v onto S_h. The condition $u_r(0,t)=0$ is not imposed on the subspace and disappears from the variational formulation. It is not hard to see that the solution $u_h(t)$ of the system of ordinary differential equations represented by (2.4) exists at least locally and satisfies the conservation laws (2.2) and (2.3) with v replaced by v_h.

We shall discretize (2.4) in the temporal variable by the *midpoint rule* as follows. Let k be the (constant for the time being) time step and let $t^n=nk, n=0,1,\dots,J$, where $Jk=T$. We seek $U^n\in S_h$, approximating $u_h(t^n)$, and satisfying for $n=0,1,\dots,J-1$ and all $\chi\in S_h$ the equation

$$(U^{n+1}-U^n,\chi)+\mathrm{i}k\varepsilon\left(\Big(\frac{U^{n+1}+U^n}{2}\Big)_r,\chi_r\right)=\mathrm{i}k\left(\left|\frac{U^{n+1}+U^n}{2}\right|^2\frac{U^{n+1}+U^n}{2},\chi\right), \tag{2.5}$$

where $U^0=v_h$. In (2.5) we solve for $V^n=\frac12(U^{n+1}+U^n)$ that satisfies

$$(V^n,\chi)+\frac{\mathrm{i}k\varepsilon}{2}(V^n_r,\chi_r)=\frac{\mathrm{i}k}{2}\left(|V^n|^2V^n,\chi\right)+(U^n,\chi),\ \forall\chi\in S_h, \tag{2.5$'$}$$

and then compute $U^{n+1}=2V^n-U^n$. On each interval Gauss numerical quadrature of sufficient high accuracy is used so that radial polynomials of degree $d+3$ are integrated exactly. The existence of solutions of the nonlinear system represented by (2.5) or (2.5′) can by readily established as in [1]. Moreover, it may be shown that this Crank–Nicolson type scheme conserves the first invariant, i.e. that there holds

$$\|U^{n+1}\|=\|U^n\|,\quad n=0,1,\dots,J-1, \tag{2.6}$$

but not the second.

To derive an estimate for the error $u(t^n)-U^n$ in L^2, we assume that the solution of (2.1) is sufficiently smooth on $[0,1]\times[0,T]$. Then, arguing along the lines of [1] we may prove that

there exists a unique solution $\{U^n\}_{n=0}^J$ of the fully discrete scheme (2.5) satisfying

$$\max_{0\le n\le J} \|u(t^n) - U^n\| \le c(k^2 + h^2), \tag{2.7}$$

provided k is sufficiently small and that $k = o(h^{d/4})$ as $h \to 0$. In (2.7) c is a constant independent of the discretization parameters. The proof makes use of the inverse inequality $\|\chi\|_{L^\infty} \le ch^{-d/2}\|\chi\|$, which is valid for $\chi \in S_h$ in view of our quasiuniformity assumption on the spatial mesh. See, however, [46] for an error estimate for the semidiscrete approximation, in which quisiuniformity is replaced by a weaker condition.

In order to solve, at each time step, the $\dim S_h \times \dim S_h$ nonlinear system of equations represented by (2.5′) one may use Newton's method or modified versions thereof, cf. [1], [2]. Here we adopt a much simpler iterative scheme, an explicit–implicit method in which the linear, resp. nonlinear, terms in (2.5′) are evaluated at the iteration levels $\ell + 1$, resp. ℓ. Given U^n and a starting value V_0^n we solve for V_ℓ^n, satisfying for all $\chi \in S_h$ and $\ell = 0, 1, \dots, \ell_n - 1$ the equations

$$(V_{\ell+1}^n, \chi) + \frac{\mathrm{i}k\varepsilon}{2}\left(V_{\ell+1,r}^n, \chi_r\right) = \frac{\mathrm{i}k}{2}\left(|V_\ell^n|^2 V_\ell^n, \chi\right) + (U^n, \chi). \tag{2.8}$$

For $n \ge 1$ we take $V_0^n = \frac{3}{2}U^n - \frac{1}{2}U^{n-1}$ as starting value and perform two iterations (i.e. $\ell_n = 2$). At $n = 0$, to compensate for the less accurate starting value $V_0^0 = U^0 = v_h$ we need $\ell_0 = 3$. Following the analysis of [2] we may show that the resulting linearized fully discrete scheme is stable and produces approximations to $u(t^n)$ that are denoted again by U^n, are defined by $U^n := 2V_2^{n-1} - U^{n-1}$ for $n \ge 1$, and satisfy the error estimate (2.7) provided again that k is sufficiently small and $k = o(h^{d/4})$ as $h \to 0$.

Therefore, if we equip S_h with its usual hat function basis, we see that by solving two tridiagonal complex linear systems at each time step, we may approximate to second order accuracy the solution of (2.1). In the code we solve the systems by the appropriate Linpack routine. The overall scheme is practically unconditionally stable as the mild mesh condition $k = o(h^{d/4})$ is probably due just to technical requirements of the convergence proof. Of course, the linearized fully discrete scheme is no longer conservative since the nonlinear system is not solved exactly. However, we found that the L^2 norm of U^n was conserved to a satisfactory degree of accuracy even in the blow-up examples; cf. Sections 4 and 5.

3. ADAPTIVE MESH REFINEMENT FOR THE APPROXIMATION OF BLOW-UP

In this section we shall describe the adaptive mechanism that we used to follow the development of point blow-up singularities of solutions of (2.1). We consider the simple base scheme (2.5). Anticipating that the solution blows up at $r = 0$ as t approaches a finite value $t^\star$, we implemented (2.5) in an adaptive code using a spatial and temporal mesh that can change with n. As the blow-up time is approached and the solution grows in amplitude near the origin, the adaptive mechanism refines drastically the spatial mesh in a neighborhood of $r = 0$ and cuts the time step by enforcing two refinement criteria that appeared to be successful for the problem at hand and will be described presently.

If the spatial mesh must be refined, then the number of nodes r_i is increased as follows: Let N and $M < 2N$ be given integers (M even) and $h = 1/N$ be the initial spatial meshlength. At the first spatial refinement we partition $[0, 1]$ as $I_0 \cup I_1$, where $I_0 = [0, Mh/2)$ and $I_1 = [0, 1]\setminus I_0$, i.e. so that I_0 consists of M subintervals of length $h/2$ and I_1 of $N - M/2$ subintervals of length h. Suppose now that the spatial grid has already been refined NSPLIT ≥ 1 times. Then, $[0, 1]$ is partitioned in NSPLIT + 2 adjacent successive intervals $I_0, I_1, \dots, I_{\mathrm{NSPLIT}+1}$ such that the

left-hand boundary of I_0 is 0, the right-hand boundary of $I_{\text{NSPLIT}+1}$ is 1, and, on each I_j the mesh is uniform, so that:
I_0 consists of M subintervals of constant meshlength $h/2^{\text{NSPLIT}+1}$.
I_1 consists of $\frac{M}{2}$ subintervals of constant meshlength $h/2^{\text{NSPLIT}}$.
I_2 consists of $\frac{M}{2}$ subintervals of constant meshlength $h/2^{\text{NSPLIT}-1}$.

$\vdots$

I_{NSPLIT} consists of $\frac{M}{2}$ subintervals of constant meshlength $h/2$.
$I_{\text{NSPLIT}+1}$ consists of $N - \frac{M}{2}$ subintervals of constant meshlength h.

As an example, starting with $N = 1600$ subintervals, i.e. an initial meshlength $h = 1/1600 = 0.625 \times 10^{-3}$, supposing that the finest mesh region has $M = 200$ subintervals and assuming that the spatial grid has been refined NSPLIT $= 34$ times, we end up with a grid consisting of $N + \frac{M}{2}(\text{NSPLIT} + 1) = 5100$ subintervals. The coarsest mesh region I_{35} has 1500 subintervals of width $h = 0.625 \times 10^{-3}$, whilst the finest mesh region I_0 consists of 200 subintervals of width $h/2^{35} \cong 0.182 \times 10^{-15}$. Each time the grid is refined I_0 is cut in half into two new intervals that are labeled I_0 and I_1, and all other regions are redefined so that I_1 becomes I_2, I_2 becomes I_3, etc.. U^n is embedded in the new mesh by linear interpolation.

The signal to perform this spatial grid refinement (i.e. to increase NSPLIT by 1) at a certain time step n is given whenever

$$\frac{\|U^n\|_{L^\infty(I_0)} h_{\min}^{1/2}}{\left(\int_{I_0} |U^n|^2 dr\right)^{\frac{1}{2}}} > \text{TOL}_h. \tag{3.1}$$

Here TOL_h is an empirically determined tolerance, usually taken to be equal to 0.12 for $d = 2$ and from 0.12 to 0.14 for $d = 3$, and $h_{\min}$ is the gridsize on I_0, which is the interval of finest mesh. The criterion (3.1) is motivated by a local $L^\infty - L^2$ inverse property that elements of the finite element subspace satisfy on I_0. The inverse property shows that the growth of the L^∞ norm is limited by the size of $h_{\min}$ and the L^2 norm of the solution on I_0 which, close to blow-up, is not changing rapidly. Hence, refining the mesh in the vicinity of $r = 0$ to satisfy (3.1), allows the amplitude of the solution to grow there. The number of subintervals M in I_0 should be chosen so as to allow a sufficiently large neighborhood of the peak to be captured in the finest mesh region. On the other hand, the computational cost of the scheme increases with M. In the case of NLS we found that $M = 200$ was a reasonable compromise. (The choice of TOL_h depends on M; the values that we used were found experimentally and correspond to $M = 200$.)

The time step reduction is motivated by a need to control, to a certain degree, changes in a scaled version of the second invariant of the problem from one time step to the next. Specifically, the time step size k is halved and the time step computation is repeated whenever

$$\frac{|H(U^{n+1}) - H(U^n)|}{1 + \int_0^1 |U_r^{n+1}|^2 r^{d-1} dr} > \text{TOL}_k/2. \tag{3.2}$$

In (3.2) $H(\cdot)$ is the Hamiltonian, defined by (2.3), and TOL_k is an empirically chosen parameter with values that ranged from 10^{-5} to 10^{-8}. These values for TOL_k and TOL_h proved successful in causing the adaptive mechanism to reduce the time step size and refine the spatial grid at suitable rates, allowing accurate simulation of the development of the blow-up. However, since the Hamiltonian is the difference of two quantities that both blow up, its computation becomes less and less accurate as we approach blow-up. The criterion (3.2) attempts to preserve the

Hamiltonian locally, i.e. from one time step to the next, but is rather ineffective in maintaining its value globally.

With any specific choice of (fixed) adaptive refinement parameters there always exists a temporal instance by which the refinements have produced grids that do not permit further growth of the amplitude of the numerical solution near the origin. This happens, most probably, when the Hamiltonian is being computed too inaccurately. The code then proceeds to cut the time step several times instead of refining in space. (The latter would have probably allowed the code to compute $H(\cdot)$ more accurately and thus make progress; instead, the time steps get cut too drastically and the peak does not increase.) A computation is stopped therefore, when a combination of these two phenomena (amplitude not strictly increasing, excessive time step cutting between spatial refinements) is observed. The numerical 'blow-up time' $t^\star$ is then defined as the instance of the last spatial grid refinement. (For another way of estimating $t^\star$, cf. Section 6.)

In the two sections that follow we report on the numerical results that we obtained approximating the rates of growth of the amplitude at the origin and of various norms of the solution and its radial derivative, as well as rates of blow-up of the phase of the solution as $t \to t^\star$. Having in mind that exceedingly large quantities will develop and their rapid evolution will have to be followed over extremely small temporal increments, we have coded our method carefully so as to minimize the effect of roundoff errors and maintain stability in the floating point arithmetic. Evidence of that is the stability of most of the blow-up rate information to be presented in the sequel. As a rule, approximate values of the various rates appear quite early in the computations. But one needs to integrate extremely close to the true blow-up time in order to attain the extra few digits, which is only possible when the computations are close to the asymptotic regime.

An example of a typical post-processing operation that is repeatedly performed is computing quantities of the form $F(t^\star - t)$ for t extremely close but less than the numerical blow-up time $t^\star$. F is evaluated at $t^\star - t_i$, $i = 1, 2, \ldots$, where t_i is the time when the i^{th} spatial grid refinement takes place. Since $t^\star - t_i$ can become e.g. of $O(10^{-20})$, it is computed as $\sum_{j=1}^{N_i} k_j n_j$ where k_j is the size of a temporal step, n_j is the number of temporal steps of size k_j, and N_i is the number of temporal steps of different size taken between t_i and $t^\star$; the sum is computed from smallest to largest terms. Details on computing particular blow-up rates will be given at the appropriate places in the next two sections.

Most computations to be reported in the sequel were performed with a double precision Fortran 77 code on a SparcClassic Sun workstation. They were not especially time consuming: A run in 2 dimensions that started with 1600 spatial mesh intervals, and reached an amplitude of $.985 \times 10^{16}$ after the spatial mesh was refined 50 times, took 9850 total cpu seconds.

4. BLOW-UP: THE THREE-DIMENSIONAL CASE

As was stated in the Introduction, there is a wealth of evidence on the dynamics of blow-up (collapse) of radially symmetric solutions of the NLS in three dimensions; the reader is referred to the papers [34] and [27] for detailed expositions and further references. In [34] it was concluded that solutions emanating from several types of initial profiles evolve into a self-similar form which blows up as $t \uparrow t^\star$ according to the law

$$u(r,t) \sim \frac{1}{(t^\star - t)^{\frac{1}{2}}} Q\Big(\frac{\sqrt{\kappa} r}{(t^\star - t)^{\frac{1}{2}}}\Big) \mathrm{e}^{\mathrm{i}\kappa(\ln \frac{1}{t^\star - t})}, \tag{4.1}$$

that had been predicted earlier by Zakharov. The blow-up time $t^\star$ depends on the initial condition, while the complex-valued function $Q(\xi)$, $\xi \in (0, \infty)$, and the real number κ solve an

'eigenvalue' problem for a nonlinear ordinary differential equation. Q and κ are independent of the initial profile that produced (4.1), and the value of κ is approximately equal to 0.545. The results of [27] are in good agreement with those of [34]. It seems, therefore, that approximating accurately the main features of (4.1) is a good benchmark for a direct integration code such as the one described in this paper. As a test of the code we approximated the blow-up of solutions emanating from several Gaussian and 'ring' type initial profiles.

A typical such example, labeled G3, corresponds to an initial value $u^0(r) = 6\sqrt{2}\mathrm{e}^{-r^2}$ on $[0,\infty)$, restricted to the interval $[0,R]$ with $R=5$, and scaled to $[0,1]$ as

$$v(r) = 6\sqrt{2}\mathrm{e}^{-25r^2}, \quad 0 \le r \le 1, \tag{4.2}$$

in the notation of (2.1). Hence $\varepsilon = 1/25$, and the Hamiltonian (2.3) is equal to about -0.87783. (This example has been considered in [34] and elsewhere. The actual value of the initial amplitude that we used was 8.485281374.) We approximated the solution using initially the spatial meshlength $h = 10^{-3}$ (i.e. $N = 10^3$) and a time step $k = 10^{-4}$. The number of intervals in the finest mesh region in this and all other experiments to be reported in the sequel was 200. The parameters in the mesh refinement criteria were $\mathrm{TOL}_h = 0.14$ and $\mathrm{TOL}_k = 5 \times 10^{-8}$. By the final, 'blow-up' time $t^\star \approx 0.03429946$, the amplitude at $r = 0$ had risen to approximately $.661 \times 10^{12}$ (thus exceeding its initial value by a factor of $.779 \times 10^{11}$), and the code had refined NSPLIT $= 35$ times the spatial mesh; the final time step used was about $.847 \times 10^{-25}$. In this computation the L^2 norm of the discrete solution (equal to about .3003974) was conserved to 7 digits up to the time of the first spatial mesh refinement. Subsequently, it approached fast a constant value to machine accuracy: For example, between the times of the 22^{nd} and the last (35^{th}) spatial mesh refinement it was constant to 15 digits.

The evolution of the magnitude of the solution is shown in Figures 1 and 2. The early stages of the development, showing the fast collapse at $r = 0$, appear in the four snapshots of Fig. 1, the first of which is the initial profile. The remaining three show the modulus of the solution as a function of r at $t = t_i, i = 1, 2, 3$, where t_i denotes the temporal instance of the i^{th} spatial refinement. Figure 2 shows, superimposed in one graph, four later stages of the evolution of the dynamically scaled modulus $|u|(t^\star - t)^{1/2}$ of the solution vs. $r/(t^\star - t)^{1/2}$ at $t = t_i, i = 4, 9, 14$ and 19. The last three profiles practically coincide, within graph thickness; the observed fast convergence confirms the validity of the self-similar form (4.1) of the blow-up for $|u|$.

We report now on the various blow-up *rates* that were computed from the output of the run G3. The amplitude magnification factors achieved in this and other similar examples are very large, and this gives us confidence that the rate computations are accurate. One group of data concerns observed blow-up rates as $t \to t^\star$, for several spatial norms of the solution or (2.1) and its first radial derivative. Let $A(t)$ be the value at time t of such a norm of $u(\cdot, t)$ or $u_r(\cdot, t)$. With output generated by the code we calculated $A(t)$ for t very close to $t^\star$ and estimated the numbers ρ such that

$$A(t) \sim (t^\star - t)^{-\rho} \text{ as } t \uparrow t^\star. \tag{4.3}$$

Specifically, we evaluate $A(t)$ at the instances $t = t_i$, $i = 1, 2, 3, \ldots$, of the i^{th} spatial refinement. Then, approximations ρ_i to the blow-up rate ρ of $A(t)$ are computed by the formula

$$\rho_i = -\ln \frac{A(t_i)}{A(t_{i+1})} / \ln \frac{t^\star - t_i}{t^\star - t_{i+1}}, \tag{4.4}$$

where the quantities $t^\star - t_i$ are evaluated in the manner explained in Section 3. In Table 1 we show the computed blow-up rates of the L^4 and L^∞ norm (i.e. of the amplitude), as well as of the L^2 and L^∞ norm of u_r in the columns labeled L^2_D and L^∞_D. (The L^∞ and L^∞_D are discrete maximum norms calculated over all quadrature points.)

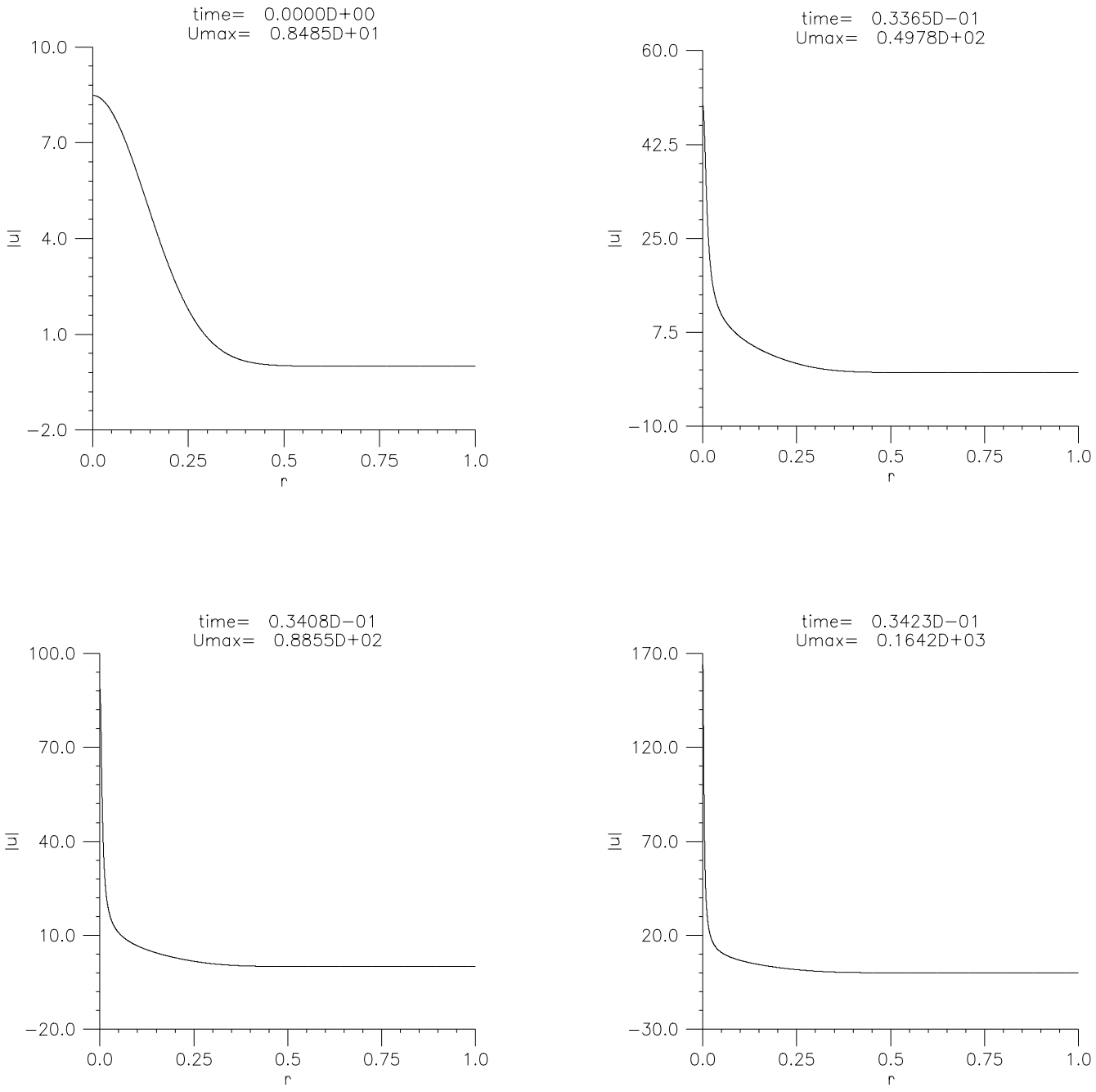

FIGURE 1. Blow-up of the modulus of the solution of example G3. Early stages.

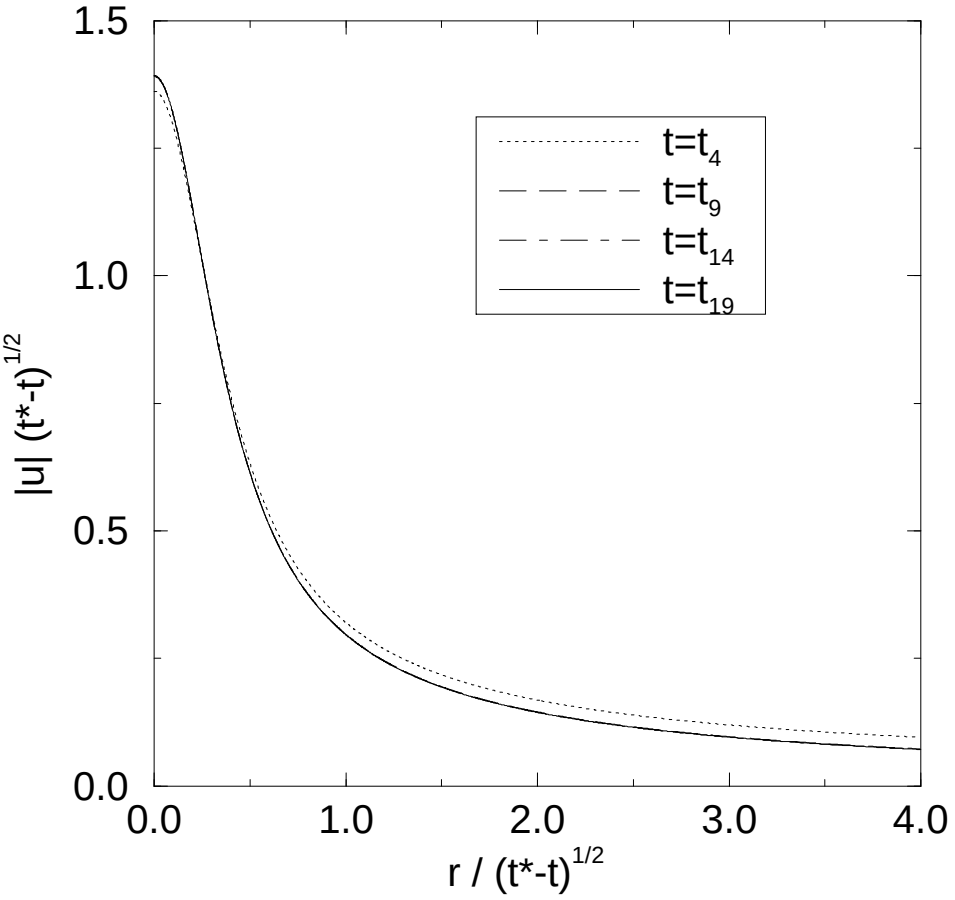

FIGURE 2. Blow-up of the modulus of the solution of example G3. Later stages.

The blow-up rates stabilize early in the computation and are quite robust. The law $(t^\star - t)^{-\frac{1}{2}}$ for the amplitude is clearly verified. The L^4 norm of u and the L^2 and L^∞ norms of u_r are seen to blow up at the rates $\rho = 1/8, 1/4$ and 1, respectively, which are of course consistent with the rates that may be computed using formula (4.1).

In the last column of Table 1, labeled κ, we list approximations, obtained from the data at $t = t_i$, of the constant κ appearing, e.g., in the exponential term $\mathrm{e}^{\mathrm{i}\kappa \ln \frac{1}{t^\star - t}}$ of (4.1). We assumed that the phase of the solution at $r = 0$ is of the form $\kappa \ln \frac{1}{t^\star - t}$ and computed values of κ at $t = t_i$ by forming the quotient $\sigma_i = U(0, t_{i+1})/U(0, t_i)$, where $U(r, t)$ is the fully discrete approximation produced by the code, then computing $\varphi_i = \arctan(\mathrm{Im}(\sigma_i)/\mathrm{Re}(\sigma_i))$ (or as $\varphi_i + \pi$ if φ_i is negative), and finally letting

$$\kappa_i = \varphi_i / \ln \frac{t^\star - t_i}{t^\star - t_{i+1}}. \tag{4.5}$$

The entries κ_i of the last column of Table 1 show that the phase constant has stabilized and that its value agrees well with 0.545, the number obtained in [34] and [27].

In Table 1 the rates are shown at the times $t_i, i = 10, 11, \ldots, 27$. (The actual values of t_i are not listed, being very close to $t^\star$.) For values of $t_i, i \geq 28$, and up to $t^\star$ (recall that $t^\star = t_{35}$ in this example), the peak of the amplitude of the solution continues to grow, but the numerical

i	L^4	L^∞	L^2_D	L^∞_D	κ
10	.12385	.50041	.24827	1.00052	.54528
11	.12438	.49972	.24904	.99966	.54532
12	.12467	.50010	.24948	1.00049	.54525
13	.12482	.50035	.24972	.99983	.54473
14	.12490	.49990	.24984	1.00072	.54518
15	.12495	.49996	.24992	.99956	.54518
16	.12497	.49976	.24996	.99959	.54516
17	.12499	.50007	.24998	1.00024	.54510
18	.12499	.50036	.24999	.99981	.54478
19	.12500	.49964	.24999	1.00079	.54535
20	.12500	.50019	.25000	.99962	.54496
21	.12500	.49986	.25000	.99927	.54495
22	.12500	.50032	.25000	1.00083	.54515
23	.12500	.49985	.25000	1.00009	.54502
24	.12500	.50021	.25000	.99954	.54519
25	.12500	.49965	.25000	1.00067	.54509
26	.12500	.50009	.24999	.99960	.54506
27	.12500	.49994	.24999	.99937	.54485

TABLE 1. Blow-up rates, G3

	$G3$	$h = 0.5 \cdot 10^{-3}$	$k = 0.5 \cdot 10^{-5}(1)$	$k = 0.5 \cdot 10^{-5}(2)$	$k = 0.5 \cdot 10^{-5}(3)$
$\lvert u\rvert_{\max}$	0.66×10^{12}	0.66×10^{12}	0.41×10^{11}	0.33×10^{12}	0.13×10^{13}
$t^\star$	.03429946	.03430110	.03429835	.03429835	.03429835

	$\mathrm{TOL}_h = 0.13$	$\mathrm{TOL}_h = 0.15$	$\mathrm{TOL}_k = 4.5 \times 10^{-8}$	$\mathrm{TOL}_k = 5.5 \times 10^{-8}$
$\lvert u\rvert_{\max}$	0.56×10^{12}	0.76×10^{12}	0.33×10^{12}	0.13×10^{13}
$t^\star$	.03429947	.03429879	.03429882	.03429942

TABLE 2. Dependence of $|u|_{\max}$ and $t^\star$ on computational parameters. (Data for G3: $h = 10^{-3}, k = 10^{-4}, \mathrm{TOL}_h = 0.14, \mathrm{TOL}_k = 5 \times 10^{-8}$)

blow-up rates deteriorate as their computation from formulas like (4.4) and (4.5) loses accuracy due to the extreme proximity of these t_i to $t^\star$.

To give the reader an idea of the degree of dependence of some numerical blow-up quantities on the initially set computational parameters of the run, we list in Table 2 the values of $|u|_{\max}$, the maximum amplitude achieved, and $t^\star$ for the run G3 and eight other runs obtained from G3 by varying each time the indicated parameter. (The three runs with the same initial time step $k = 0.5 \times 10^{-5}$, correspond, respectively, to allowing a maximum number of $3000, 3200$ and 3400 time steps; the standard G3 had 3000 time steps. When halving the initial k it is advisable to allow perhaps a 10% or so extra steps to ensure that the run will get far enough in the blow-up regime.) In all these runs the evolution and the values of the computed rates of blow-up were very similar to those of G3 shown in Table 1.

In addition to examples with Gaussian initial data we also ran exponentially decaying 'ring'-type initial profiles of the form $v(r) = ae^{-br}(1+c_1 r+c_2 r^2), 0 \le r \le 1$, having a single maximum

at some $0 < r < 1$. These 'rings' collapsed relatively fast at zero; the observed values of norm blow-up rates and κ were practically the same (albeit slightly more stabilized) with the G3 values of Table 1.

5. BLOW-UP: THE CRITICAL CASE

In this section we report the results of numerical experiments that we performed with our adaptive code in the critical, two-dimensional case. We computed blow-up rates for the amplitude of the solution of (1.2) at $r = 0$, as well as for several of its norms and norms of its radial derivative. We also computed a certain constant occurring in the expression of the phase of the solution at $r = 0$.

There exists by now strong evidence from numerical computations and asymptotic calculations (see the discussion and the references quoted in the Introduction) suggesting that the amplitude $A(t)$ of the solution at $r = 0$ behaves basically like $(t^\star - t)^{-\frac{1}{2}}$ as $t \uparrow t^\star$ but is perturbed (slowed down) by a factor that tends slowly to infinity as $t \uparrow t^\star$. One may write then that

$$A(t) \sim \left(\frac{F(t^\star - t)}{t^\star - t}\right)^{\frac{1}{2}} \text{ as } t \uparrow t^\star, \tag{5.1}$$

where the function $F(s)$, defined for $s > 0$, tends to infinity as $s \downarrow 0$ slower than any power of s. Several choices of F have been made in the literature, e.g., $F(s) = \ln \frac{1}{s}$, [48], [50], $F(s) = \left(\ln \frac{1}{s}\right)^\gamma$, $0.35 \le \gamma \le 0.65$, [27], $F(s) = \ln \ln \frac{1}{s}$, [28], [32], [19].

We shall compare these amplitude blow-up laws against numerical results obtained from our adaptive code. As in Section 4 we experimented with radially exponentially decreasing (Gaussian, ring) initial profiles. Our first family of examples are Gaussians of various amplitudes. We took, in the notation of (2.1) with $d = 2$,

$$v(r) = A_0 \mathrm{e}^{-25r^2}, \quad 0 \le r \le 1, \tag{5.2}$$

using the scaling factor $\varepsilon = 1/25$ and several values of A_0. We denote these examples as (G2, A_0) in the sequel.

In the case $A_0 = 6\sqrt{2}$ (actually $A_0 = 8.485281374$), the Hamiltonian (2.3) being equal to about -11.520, we started with initial mesh sizes $h = 1/1600$, $k = 0.8 \times 10^{-4}$. With refinement criteria parameters $\mathrm{TOL}_h = 0.12$ and $\mathrm{TOL}_k = 3 \times 10^{-8}$, the code was able to perform 34 spatial grid refinements; at the final ('blow-up') time $t^\star \approx 0.040289800$ it had achieved an amplitude at $r = 0$ equal to about $.258 \times 10^{12}$, the last time step being equal to about 0.108×10^{-23}. In this computation the L^2 norm of the discrete solution (equal to about 0.848528) was conserved to 6 digits up to the time of the seventh spatial mesh refinement. Subsequently, it was conserved to 5 digits. Output from this run as well as from other similar runs with different A_0 served to approximate numerically various blow-up quantities. First, we describe our results on the blow-up rates of the amplitude $A(t)$ of the solution at $r = 0$. We computed approximations to the power $\rho > 0$ (ρ should be close to 1/2 by (5.1)) assuming that the numerically computed amplitude at $r = 0$ behaves like

$$A(t) \sim [F(t^\star - t)/(t^\star - t)]^\rho \text{ as } t \uparrow t^\star, \tag{5.3}$$

where $F(s)$, $s > 0$, is one of the six laws

$$F(s) = \left(\ln \frac{1}{s}\right)^\gamma, \quad \gamma = 1, 0.6, 0.5, 0.4, 0, \tag{5.3a}$$

$$F(s) = \ln \ln \frac{1}{s}. \tag{5.3b}$$

As in the experiments of the previous section, for $i = 1, 2, 3, \ldots$, we computed $A_i = A(t_i)$, the value of A at the time t_i of the i^{th} spatial refinement. We then calculated approximations ρ_i of ρ by the formula

$$\rho_i = \ln\left(\frac{A_i}{A_{i+1}}\right) / \ln\left(\frac{F_i/(t^\star - t_i)}{F_{i+1}/(t^\star - t_{i+1})}\right), \tag{5.4}$$

where $F_i = F(t^\star - t_i)$. Table 3 shows ρ_i for $14 \le i \le 28$ (the quality of the computed ρ_i's degenerated for $i > 28$ due to the extreme proximity of those t_i to $t^\star$). The results for the choices (5.3a,b) for $F(s)$ appear in the columns labeled $\gamma = 1, 0.6, \ldots, 0, \log\log$, respectively.

The last four rows of each column of the table show some statistics of the rates of that column, computed using the values of the data at t_i in the window $k = 19$ to $\ell = 28$ closer to the asymptotic regime. (We use the notation $.698(-3) = .698 \times 10^{-3}$ etc.). In addition to the mean and standard deviation of the data for the window $[19, 28]$ we show the 'ℓ_1 discrepancy' defined for the window $[k, \ell]$ as

$$\varepsilon_1 := \frac{1}{\ell - k + 1} \sum_{i=k}^{\ell} |\frac{1}{2} - \rho_i|,$$

i.e. as the scaled ℓ_1 norm of the vector $\frac{1}{2} - \rho_i, k \le i \le \ell$, and the '$\ell_2$ discrepancy'

$$\varepsilon_2 := \big[\frac{1}{\ell - k + 1} \sum_{i=k}^{\ell} \big(\frac{1}{2} - \rho_i\big)^2\big]^{1/2},$$

i.e. the corresponding scaled ℓ_2 norm of the same vector.

As expected, all laws (5.3a,b) when substituted in (5.3), yield rates close to 0.5. The rates of the column corresponding to the $\log\log$ rate (5.3b) clearly stabilize closer to 0.5 than any other law. The laws (5.3a) corresponding to the powers $\gamma = 0.6, 0.5$ and 0.4 give very robust rates which however cluster with small deviation around mean values that differ from 0.5 by a larger amount as compared to those of the $\log\log$ case.

This picture is reinforced by examining data from other runs corresponding to Gaussian initial profiles of different amplitudes. For example, consider the output from a run labeled (G2, 8) that corresponds to a profile of the form (5.2) with $A_0 = 8$ (Hamiltonian $= -8.96$). With initial mesh sizes $h = 1/2400$, $k = 0.75 \times 10^{-4}$ and $\text{TOL}_h = 0.12$, $\text{TOL}_k = 3.4 \times 10^{-8}$ the code was able to perform 45 refinements of the spatial grid at which point it reached the final ('blow-up') time $t^\star \approx .043706879$, achieving a maximum amplitude of about $.793 \times 10^{15}$; the last time step was approximately of size $.303 \times 10^{-31}$. With data from this run we generated Table 4, analogous to Table 3. We show the values for $18 \le i \le 32$; their quality degenerated after $i = 32$.

Since the final amplitude reached in this run was higher, we expect rates from data closer to the asymptotic regime. The rates of columns $\gamma = 0$ and $\gamma = 1$ improve slightly, while those of the columns corresponding to $\gamma = 0.6, 0.5, 0.4$ remain basically the same with their counterparts of Table 3. The $\log\log$ rates stabilize further, and their mean in the window [23,32] is closer to the expected value 0.5. Again, the values of the ℓ_1 and ℓ_2 discrepancies from 1/2 are much smaller in the $\log\log$ case. However, closer inspection of Tables 3 and 4 invites further comment.

The laws $F(s) = \big(\ln\frac{1}{s}\big)^\gamma$ were proposed in [27] as a result of numerical computations with a 'dynamic rescaling' type technique. The interval $[0.35, 0.65]$ of recommended values of γ was suggested there by curve-fitting with data from those computations. In our case, the data in Tables 3 and 4 suggest that as γ decreases from $\gamma = 1$ to $\gamma = 0$, the corresponding rates increase monotonically (as they should) from about .491 to about .503. The $\log\log$ growth, theoretically

i	$\gamma = 1$	$\gamma = 0.6$	$\gamma = 0.5$	$\gamma = 0.4$	$\gamma = 0$	$\log\log$
14	.48828	.49634	.49839	.50047	.50894	.50222
15	.48804	.49566	.49761	.49957	.50756	.50133
16	.48860	.49585	.49770	.49956	.50714	.50133
17	.48888	.49579	.49754	.49931	.50651	.50108
18	.48919	.49578	.49746	.49914	.50600	.50090
19	.48947	.49577	.49737	.49898	.50553	.50072
20	.48976	.49580	.49733	.49888	.50514	.50060
21	.49004	.49583	.49730	.49878	.50479	.50049
22	.49030	.49587	.49729	.49871	.50448	.50039
23	.49057	.49594	.49730	.49867	.50422	.50033
24	.49081	.49599	.49730	.49862	.50396	.50026
25	.49103	.49603	.49729	.49856	.50372	.50018
26	.49126	.49609	.49731	.49854	.50351	.50013
27	.49138	.49605	.49723	.49842	.50323	.49999
28	.49145	.49598	.49712	.49827	.50292	.49982
Mean [19–28]	.49061	.49593	.49729	.49864	.50415	.50029
Std. dev. [19–28]	.698(−3)	.110(−3)	.672(−4)	.211(−3)	.844(−3)	.276(−3)
ℓ_1 discr. [19–28]	.939(−2)	.407(−2)	.271(−2)	.136(−2)	.415(−2)	.329(−3)
ℓ_2 discr. [19–28]	.942(−2)	.407(−2)	.272(−2)	.137(−2)	.423(−2)	.392(−3)

TABLE 3. Blow-up rates of the amplitude $A(t)$ at $r = 0$ of (G2, $6\sqrt{2}$) corresponding to laws (5.3a,b).

slower than any power of log, is very close to 0.5. A natural question is then whether there exist values of $\gamma \in (0, 0.4)$ for which laws of the form $\big(\ln \frac{1}{s}\big)^{\gamma}$ can fit data from a particular experiment as well as the $\log\log$ law or even better.

There are many criteria of course on the basis of which data may be fitted to a particular law. We found the following procedure reasonable: Let $F_i = F(t^\star - t_i) = \big(\ln \frac{1}{t^\star - t_i}\big)^{\gamma}$, and let $\rho_i(\gamma), 0 \le \gamma \le 1$, be the corresponding rate given by (5.4). Then, a straightforward calculation yields the formula

$$\frac{1}{\rho_i(\gamma)} = \frac{\gamma}{\rho_i(1)} + \frac{1-\gamma}{\rho_i(0)}, \tag{5.5}$$

expressing the rate $\rho_i(\gamma)$ at $t = t_i$ obtained from the '$\gamma-$law' $\big(\ln \frac{1}{s}\big)^{\gamma}$, in terms of the rates $\rho_i(1)$ and $\rho_i(0)$, corresponding to the laws $F(s) = \ln \frac{1}{s}$ and $F(s) = 1$, respectively. One may then compute with a standard root finder, given a set of rates $\{\rho_i(1), \rho_i(0)\}, k \le i \le \ell$, a value $\gamma = \gamma^\star$ that minimizes over $\gamma \in [0, 1]$ the scaled ℓ_2 norm

$$\varepsilon_2(\gamma) = \big[\frac{1}{\ell - k + 1} \sum_{i=k}^{\ell} \big(\frac{1}{2} - \rho_i(\gamma)\big)^2\big]^{1/2}$$

of the vector $\frac{1}{2} - \rho_i(\gamma), k \le i \le \ell$, and compare $\varepsilon_2(\gamma^\star)$ with $\varepsilon_2(\log\log)$, the latter being the analogous quantity computed using the $\log\log$ rates ρ_i, i.e. the entries of the last columns of

i	$\gamma = 1$	$\gamma = 0.6$	$\gamma = 0.5$	$\gamma = 0.4$	$\gamma = 0$	$\log\log$
18	.48929	.49571	.49734	.49898	.50566	.50073
19	.48958	.49572	.49728	.49885	.50524	.50059
20	.48986	.49576	.49726	.49876	.50487	.50047
21	.49017	.49583	.49727	.49871	.50458	.50041
22	.49041	.49586	.49724	.49863	.50427	.50031
23	.49068	.49593	.49726	.49860	.50403	.50025
24	.49093	.49600	.49728	.49857	.50380	.50020
25	.49116	.49606	.49730	.49855	.50360	.50015
26	.49140	.49614	.49734	.49854	.50342	.50012
27	.49162	.49621	.49737	.49854	.50326	.50010
28	.49182	.49627	.49739	.49852	.50309	.50006
29	.49201	.49633	.49742	.49851	.50294	.50003
30	.49221	.49640	.49746	.49853	.50282	.50001
31	.49238	.49645	.49748	.49852	.50269	.49998
32	.49254	.49650	.49750	.49851	.50256	.49995
Mean [23–32]	.49168	.49623	.49738	.49854	.50322	.50009
Std. dev. [23–32]	.630(−3)	.196(−3)	.848(−4)	.297(−4)	.488(−3)	.971(−4)
ℓ_1 discr. [23–32]	.832(−2)	.377(−2)	.262(−2)	.146(−2)	.322(−2)	.991(−4)
ℓ_2 discr. [23–32]	.834(−2)	.377(−2)	.262(−2)	.146(−2)	.325(−2)	.126(−3)

TABLE 4. Blow-up rates of the amplitude $A(t)$ at $r = 0$ of (G2, 8) corresponding to laws (5.3a,b).

k	$\gamma^\star$	$\varepsilon_2(\gamma^\star)$	$\varepsilon_2(\log\log)$
14	.341	.725(−3)	.892(−3)
15	.330	.573(−3)	.708(−3)
16	.323	.525(−3)	.636(−3)
17	.316	.453(−3)	.540(−3)
18	.309	.395(−3)	.461(−3)
19	.303	.344(−3)	.392(−3)
20	.298	.303(−3)	.336(−3)
21	.293	.269(−3)	.286(−3)
22	.288	.240(−3)	.243(−3)
23	.283	.218(−3)	.208(−3)
24	.278	.194(−3)	.173(−3)

TABLE 5. $\gamma^\star, \varepsilon_2(\gamma^\star)$ and $\varepsilon_2(\log\log)$ for window $[k, 28]$. Data of Table 3 ((G2, $6\sqrt{2}$)).

Tables 3 and 4. For example, using the data of Table 3 we tabulate in Table 5, for the windows $[k, \ell]$ with $\ell = 28$ and $k = 14, \ldots, 24$, the corresponding values of $\gamma^\star$, $\varepsilon_2(\gamma^\star)$ and $\varepsilon_2(\log\log)$.

The values of $\gamma^\star$ decrease monotonically from .341 to .278 as the size of the window $[k, 28]$ decreases, i.e. as we get closer to the 'asymptotic' regime. So do the values of $\varepsilon_2(\gamma^\star)$ and

k	$\gamma^\star$	$\varepsilon_2(\gamma^\star)$	$\varepsilon_2(\log\log)$
18	.297	.340(−3)	.318(−3)
19	.291	.293(−3)	.265(−3)
20	.287	.253(−3)	.223(−3)
21	.283	.220(−3)	.187(−3)
22	.279	.186(−3)	.152(−3)
23	.276	.161(−3)	.126(−3)
24	.273	.138(−3)	.103(−3)
25	.270	.118(−3)	.827(−4)
26	.267	.101(−3)	.669(−4)
27	.264	.846(−4)	.521(−4)
28	.262	.671(−4)	.376(−4)

TABLE 6. $\gamma^\star, \varepsilon_2(\gamma^\star)$ and $\varepsilon_2(\log\log)$ for window $[k, 32]$. Data of Table 4 ((G2, 8)).

$\varepsilon_2(\log\log)$. The values of $\varepsilon_2(\gamma^\star)$ are smaller than the corresponding values of $\varepsilon_2(\log\log)$ until we get close enough to the asymptotic regime where the $\log\log$ entries become smaller. When we use data from Table 4, i.e. from the run of the example (G2, 8) which achieved a higher final amplitude, performed more spatial refinements, and is therefore expected to have produced data much closer to the asymptotic regime, we obtain Table 6, analogous to Table 5. Now all the $\varepsilon_2(\log\log)$ entries are smaller than those of $\varepsilon_2(\gamma^\star)$ for the corresponding window. Note also that eventually the $\gamma^\star$'s of Table 6 are smaller than those of Table 5.

The results from other data fitting exercises that we also used to construct 'good' values of γ were qualitatively the same. The following picture emerges: For a given numerical experiment, there exists a range of values of γ giving laws of the type $\left(\ln\frac{1}{s}\right)^\gamma$ that fit the amplitude blow-up data quite well. However, as we get closer to the asymptotic regime our numerical experiments indicate that the $\log\log$ law has the advantage.

As in the three-dimensional case, the code also generates approximations to the blow-up rates of several other norms of the solution and its radial derivative. As an example, in Table 7 we show the temporal blow-up rates of the L^3 and L^4 spatial norms of the solution of (2.1) with initial data (G2, 8) as well as those of the L^2 and L^∞ norms of its first radial derivative; the latter appear in the columns labeled L^2_D and L^∞_D. All rates were computed with a $\log\log$ correction factor: The rates shown are approximations at $t = t_i$ of positive constants ρ, computed from values of $M(t)$ of the corresponding norm produced by the code assuming that $M(t) \sim \left[(\ln\ln\frac{1}{t^\star - t})/(t^\star - t)\right]^\rho$.

We may conclude with confidence from the results of Table 7 (and similarly robust evidence from other Gaussian and ring initial profile runs) that the blow-up rates are 1/6 for the L^3 and 1/4 for the L^4 norm of the solution, and 1/2 for the L^2 and 1 for the L^∞ norm of the radial derivative. These rates are consistent with those expected from the following asymptotic expression for u, put forth by Landman *et al.* in [28], and valid for small r as t approaches $t^\star$

$$u(r,t) \cong \frac{1}{L(t)} R\left(\frac{r}{L(t)}\right) \exp\left[\mathrm{i}\tau(t) - \frac{\mathrm{i}r^2}{8(t^\star - t)}\right], \tag{5.6}$$

where $L(t) \sim [\ln\ln\frac{1}{t^\star - t}/(t^\star - t)]^{-\frac{1}{2}}$. For characterizations of the function $R(\xi)$, $\xi \geq 0$, cf. [28], [27].

The evolution of the magnitude of the solution of $(\mathrm{G2}, 6\sqrt{2})$ as it blows up is shown in Figure 3. Superimposed in one graph we see four instances (at $t_i, i = 4, 9, 14$, and 19) of the

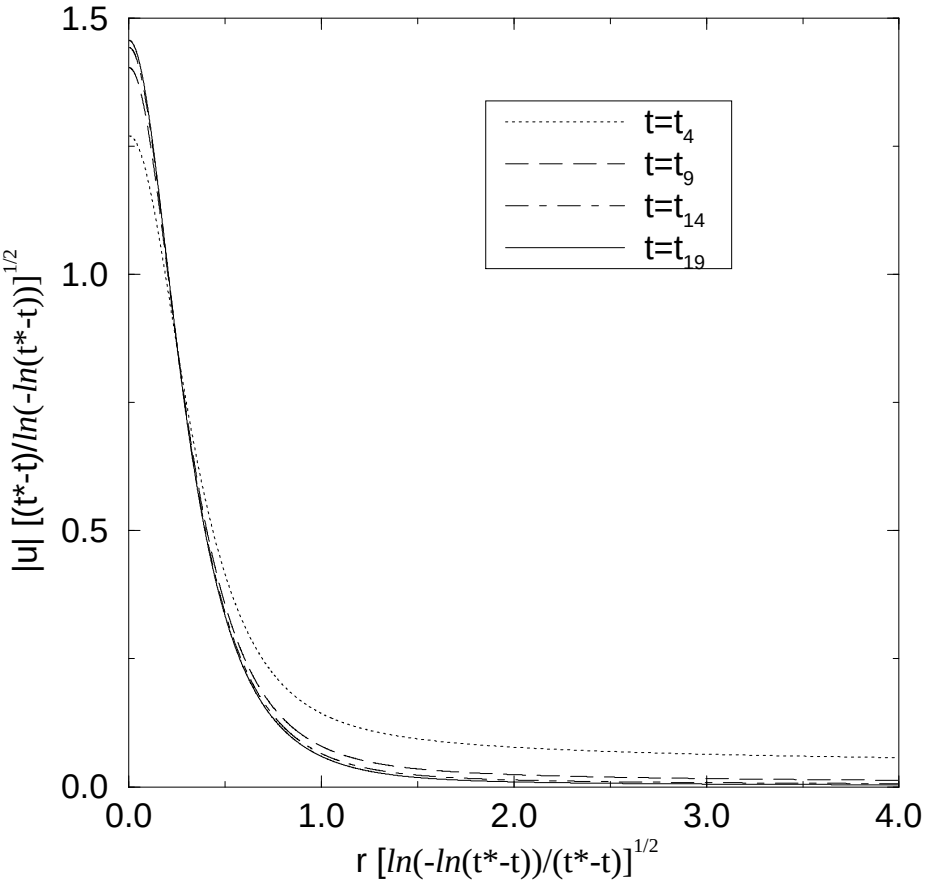

FIGURE 3. Blow-up of the modulus of the solution of example (G2, $6\sqrt{2}$).

i	L^3	L^4	L^2_D	L^∞_D
18	.16668	.25023	.50045	1.00123
19	.16666	.25017	.50035	1.00150
20	.16664	.25013	.50026	1.00113
21	.16663	.25010	.50019	1.00048
22	.16662	.25007	.50014	1.00119
23	.16661	.25004	.50009	1.00039
24	.16661	.25002	.50005	1.00032
25	.16660	.25001	.50002	1.00081
26	.16660	.24999	.49999	1.00036
27	.16660	.24998	.49997	1.00025
28	.16659	.24997	.49995	1.00017
29	.16659	.24996	.49993	.99990
30	.16659	.24995	.49991	.99981
31	.16659	.24995	.49989	1.00024
32	.16658	.24993	.49986	.99975

TABLE 7. Blow-up rates of various norms, (G2, 8).

dynamically scaled modulus $|u|/A(t)$ of the solution vs. $rA(t)$ where, motivated by (5.6), we have set $A(t) = \left[(\ln\ln\frac{1}{t^\star - t})/(t^\star - t)\right]^{1/2}$. Despite the compensating log log factor, it is evident that the evolution is now slower than in the three-dimensional case shown in Figure 2. This figure (and similar ones obtained from other initial profiles but not shown here) supports the validity of the weakly perturbed self-similar form (5.6) for the blow-up of $|u|$.

In the formula (5.6) the phase τ of the solution at $r = 0$ blows up as $t \to t^\star$. It was argued in [28] by means of asymptotic techniques that the first-order term in the asymptotic expression of $\tau(t)$ for t near $t^\star$ is given by

$$\tau(t) \cong \frac{1}{2\lambda} \ln \frac{1}{t^\star - t} \ln\ln \frac{1}{t^\star - t}, \tag{5.7}$$

where λ is a constant whose value was predicted to be $\lambda = \pi$ in [28] by means of a limiting argument of descent from the supercritical cases $d > 2$ that uses asymptotic techniques and the numerical solution of a singularly perturbed nonlinear eigenvalue problem. Later, the precise matched asymptotic analysis of [41] gave that $\lambda = \pi$ exactly.

In the dynamic rescaling framework of [28] (and also of other cited papers of the same group), (5.7) is the first-order term in the asymptotic expansion as $t \uparrow t^\star$ of $\tau(t)$ which is viewed as a transformed new temporal variable that tends to ∞ as $t \uparrow t^\star$. The exact formula for $\tau(t)$ is

$$\tau(t) = \int_0^t \frac{ds}{L^2(s)}, \quad 0 \le t < t^\star. \tag{5.8}$$

It should be noted that the amplitude of the solution $u(r,t)$ at $r = 0$ is proportional to $1/L(t)$. In turn, L is related to a quantity called $a(\tau)$ and given by

$$a(\tau) = -\frac{1}{L}\frac{dL}{d\tau}, \tag{5.9}$$

when L is considered as a function of τ. In [28] it is argued that $a(\tau)$ solves an ordinary differential equation and satisfies, to first-order terms in τ,

$$a(\tau) \cong \frac{\lambda}{\ln\tau} \quad \text{as } \tau \to \infty. \tag{5.10}$$

Using (5.10) in (5.9) an asymptotic expression may be found for $L(\tau)$, valid for large τ. Substitution in (5.8) then gives to first-order terms (5.7).

To verify computationally (by dynamic rescaling, a byproduct of which are approximations of the values of $a(\tau)$ for increasing τ) the predicted value $\lambda = \pi$, it was deemed necessary in [28] to compute $a(\tau)$ to the next-order term. This expression found was

$$a(\tau) \cong \frac{\lambda}{\ln\tau + 3\ln\ln\tau}. \tag{5.11}$$

Plotting $a(\tau)$ vs. $1/(\ln\tau + 3\ln\ln\tau)$ Landman *et al.* found that the dependence was indeed linear but that the slope was not equal to $\lambda = \pi$, presumably because τ was not large enough and the asymptotic regime in which (5.11) is valid had not been reached yet. (See also the relevant comments in [33].)

When we tested the form (5.7) versus phase output from our adaptive direct integration code for values of t close to $t^\star$, we found that the ratio $\tau(t)/\ln\frac{1}{t^\star - t}\ln\ln\frac{1}{t^\star - t}$ did not quite stabilize and took values that were near 0.36, still far from the predicted value $\frac{1}{2\pi} \cong .159$. At the suggestion of Prof. C. Sulem we tried to compare the computed values of $\tau(t)$ with an expression that includes the next term in the asymptotic expansion of $\tau(t)$ as $t \uparrow t^\star$, corresponding to the

level of (5.11). A long computation gave us the next term in the expansion; the corresponding two-term expression for $\tau(t)$ is

$$\tau(t) \cong \frac{1}{2\lambda} \ln \frac{1}{t^\star - t} \left[\ln \ln \frac{1}{t^\star - t} + 4 \ln \ln \ln \frac{1}{t^\star - t} \right]. \tag{5.12}$$

This formula was used in our calculations with the objective of recovering the constant $\frac{1}{2\lambda} =: \kappa$. Defining, as in the three-dimensional case, $\varphi_i = \arctan(\mathrm{Im}(\sigma_i)/\mathrm{Re}(\sigma_i))$, with $\sigma_i = U(0, t_{i+1})/U(0, t_i)$, we computed approximations of κ at t_i by

$$\kappa_i = \varphi_i / \ln \mu_i, \tag{5.13}$$

where $\mu_i := (t^\star - t_i)^{\alpha_i}/(t^\star - t_i)^{\alpha_{i+1}}$, $\alpha_i := \ln \ln \frac{1}{t^\star - t_i} + 4 \ln \ln \ln \frac{1}{t^\star - t_i}$.

In Table 8 we show the results of three computations of the constant κ (at times t_i of the i^{th} spatial refinement of each run as usual) from three runs, with initial data $(\mathrm{G2}, 6\sqrt{2})$, $(\mathrm{G2}, 8)$ and $(\mathrm{G2}, 4)$, respectively. The parameters of the first two runs have been already specified. The third, corresponding to initial data of the form (5.2) with $A_0 = 4$ (Hamiltonian $= -0.32$), started with $h = 1/1600$, $k = 10^{-4}$, and after performing 50 spatial refinements using $\mathrm{TOL}_h = 0.12$, $\mathrm{TOL}_k = 3.2 \times 10^{-8}$ stopped at $t^\star \approx .145445128$ achieving a maximum amplitude at $r = 0$ of $.985 \times 10^{16}$ with a final temporal step size of $.631 \times 10^{-33}$. In all three examples the phase constant was between .15 and .16, and increased slowly with i until accuracy was lost when the values of t_i became extremely close to $t^\star$. The numbers $\kappa_{i+1} - \kappa_i$ decreased monotonically from 10.6×10^{-4} to 1.6×10^{-4} for the example $(\mathrm{G2}, 6\sqrt{2})$, from 6.9×10^{-4} to 0.9×10^{-4} for (G2, 8), and, more slowly, from 4.5×10^{-4} to 2.4×10^{-4} for (G2, 4). We conclude that these computations verify quite accurately the predicted rate $\frac{1}{2\lambda} = 0.159$ of [28] and [41].

This level of accuracy is rather surprising *prima facie*, given that in the range of our computations the term $4 \ln \ln \ln \frac{1}{t^\star - t}$ in (5.12) is actually larger than $\ln \ln \frac{1}{t^\star - t}$ and that one cannot claim that the remainder after two terms of the asymptotic expansion is small. (For example, the smallest values $t^\star - t_i$ achieved by the code were $t_{34} - t_{33} \approx 0.38 \times 10^{-21}$ in the case $(\mathrm{G2}, 6\sqrt{2})$, $t_{45} - t_{44} \approx 0.33 \times 10^{-28}$ in the case $(\mathrm{G2}, 8)$, and $t_{50} - t_{49} \approx 0.35 \times 10^{-31}$ in the case $(\mathrm{G2}, 4)$; note on the other hand that $\ln \ln 10^{30} \approx 4.24$ and $4 \ln \ln \ln 10^{30} \approx 5.77$.) The matter can be clarified if one examines the next few terms in the asymptotic expansion of τ as $t \uparrow t^\star$. Tedious computations yield

$$\begin{aligned} \tau(t) \cong \frac{1}{2\lambda} \ln \frac{1}{t^\star - t} \big[& \ln \ln \frac{1}{t^\star - t} + 4 \ln \ln \ln \frac{1}{t^\star - t} - (1 + \ln 2 + 3 \ln \lambda) \\ & + 16 \frac{\ln \ln \ln \frac{1}{t^\star - t}}{\ln \ln \frac{1}{t^\star - t}} + O\Big(\frac{1}{\ln \ln \frac{1}{t^\star - t}}\Big) \big]. \end{aligned} \tag{5.14}$$

For $\lambda = \pi$, $1 + \ln 2 + 3 \ln \lambda \approx 5.13$. The fourth term in the brackets tends to zero very slowly as $t \uparrow t^\star$ and, for example, is equal to about 5.45 if $t^\star - t = 10^{-30}$. Hence, the third and fourth terms, being of opposite sign, counteract each other with the result that for $\lambda = \pi$ and, e.g., $t^\star - t = 10^{-30}$ the values of $\tau(t)$ obtained by the two-term formula (5.12) and the four-term (5.14) differ by less than 3%. So, there is hidden accuracy in (5.12), which could explain the accuracy of the computed value of λ. We think that retrieving the predicted value of λ yields more computational evidence in favor of the validity of the log log law.

Finally, we mention that, as in the three–dimensional case, we also computed with several ring type initial profiles. All blow-up rates that we found agreed to about three digits with their Gaussian counterparts of Tables 3, 4, 7 and 8.

(G2, $6\sqrt{2}$)		(G2, 8)		(G2, 4)	
i	κ_i	i	κ_i	i	κ_i
16	.14701	20	.15146	20	.15574
17	.14807	21	.15215	21	.15619
18	.14903	22	.15279	22	.15662
19	.14990	23	.15338	23	.15702
20	.15070	24	.15394	24	.15740
21	.15144	25	.15445	25	.15776
22	.15212	26	.15494	26	.15810
23	.15275	27	.15540	27	.15842
24	.15333	28	.15584	28	.15874
25	.15388	29	.15624	29	.15904
26	.15438	30	.15664	30	.15932
27	.15483	31	.15700	31	.15960
28	.15522	32	.15735	32	.15986
29	.15538	33	.15766	33	.16012
		34	.15794	34	.16037
		35	.15815	35	.16061
		36	.15824	36	.16085

TABLE 8. Constant $\kappa = 1/2\lambda$ in phase formula (5.12) from runs (G2, $6\sqrt{2}$), (G2, 8), (G2, 4).

6. CONCLUSIONS AND EXTENSIONS

In this paper we presented a direct, fully discrete, adaptive Galerkin finite element method for approximating, in two and three space dimensions, singular solutions of the radial NLS that blow up at the origin as the temporal variable t approaches some finite $t^\star$. The spatial and temporal mesh refinement adaptive techniques used allowed the numerical solutions to reach very large amplitude magnifications at the origin, for t extremely close to the blow-up time $t^\star$. On the other hand, the several computed blow-up rates were quite robust, lending support to the conclusion that the method describes accurately the characteristics of the singular solution as it blows up. Specifically, in the three-dimensional case, the numerical results clearly indicate that the solution that blows up is of self-similar form and that its amplitude at the origin blows up at the well-known rate $(t^\star - t)^{-\frac{1}{2}}$, while in the critical, two-dimensional case they are consistent with the amplitude blow-up law $\left[\ln\ln\frac{1}{t^\star - t}/(t^\star - t)\right]^{\frac{1}{2}}$ of [28], [32], [19]. In addition, the blow-up of the phase of the singular solution is accurately described in two and three dimensions.

The blow-up rates shown in the previous sections were computed with the numerical 'blow-up' time defined as $t_{i_{\max}}$, the instance of the last spatial grid refinement. We briefly indicate here another way of estimating $t^\star$ (more precisely, $t^\star - t_i$), that uses only information generated by the computer code and may sometimes improve the quality of blow-up rates. We observed that for i large enough the quantities $\omega_i = (t_{i+1} - t_i)/(t_i - t_{i-1})$ were approximately equal to $1/4$ in the case of NLS. This is consistent with the self-similar form in 3−D and the almost self-similar form of the blow-up profile in 2−D, and the fact that, as blow-up is approached, most of the solution is concentrated in the finest grid region I_0, which is halved at each t_i. If the differences $t_{i+1} - t_i$ decreased exactly geometrically, i.e. with constant ratio $\omega < 1$, instead

i	log log
25	.50019
26	.50015
27	.50006
28	.50009
29	.50007
30	.50004
31	.50003
32	.50001

TABLE 9. Blow-up rates of the amplitude $A(t)$ at $r = 0$ of $(\mathrm{G2}, 6\sqrt{2})$ corresponding to the log log law (5.36) and computed using (6.1).

of approximating $t^\star - t_i$ by $\sum_{j=i+1}^{i_{\max}}(t_j - t_{j-1})$, one could have computed $t^\star - t_i$ exactly as

$$t^\star - t_i = (t_{i+1} - t_i) + (t_{i+2} - t_{i+1}) + \cdots = (t_{i+1} - t_i)(1 + \omega + \omega^2 + \cdots) = \frac{t_{i+1} - t_i}{1 - \omega}\,.$$

However, for several reasons, e.g., the fact that the blow-up is weakly perturbed from self-similarity in 2−D, various errors of the fully discrete approximation, and some uncertainty in defining t_i as the cutting instance from inequalities like (3.1), the ratios ω_i are not exactly equal to 1/4 but usually oscillate with the tendency to approach 1/4 from above as i increases. In view of this we used the formulas

$$t^\star - t_i = (t_{i+1} - t_i) + (t_{i+2} - t_{i+1}) + \cdots + (t_{m+1} - t_m) + \frac{t_{m+2} - t_{m+1}}{1 - \bar\omega_m} \tag{6.1}$$

to estimate $t^\star - t_i$ for $i \le m \le i_{\max} - 2$, where we took $\bar\omega_m$ to be an average value of several ω_j for j near m. For example, in the test case $(\mathrm{G2}, 6\sqrt{2})$, where $i_{\max} = 34$, using (6.1) with $m = 32$ and $\bar\omega_{32} = (\omega_{32} + \omega_{33})/2 = 0.25145\ldots$ we computed the blow-up rates for the amplitude at $r = 0$. (To compute the rate ρ_{32}, $t^\star - t_{33}$ is needed; it is estimated as $(t_{34} - t_{33})/(1 - \bar\omega_{32})$.) The rates corresponding to the log log law (last column of Table 3) remained the same to five digits up to $i = 24$; for $25 \le i \le 32$ they are listed in Table 9. It is evident that in this example the new estimates of $t^\star - t_i$ permit computing good rates very close to the blow-up time. The phase constants κ_i also improve in comparison with the data of Table 8; for example $\kappa_{32} = .15689$ with the new estimates of $t^\star - t_i$. It is interesting to note that the amplitude rates of the γ−laws (5.3a) do not change much under the new procedure when compared with the values of Table 3. For example, the new rates for $i = 32$ are .49249, .49652, .49753, .49855, .50268, for $\gamma = 1, 0.6, 0.5, 0.4, 0$, respectively.

One cannot however be categorical about the effectiveness of the 'geometric tail' correction (6.1). For example, in the test case $(\mathrm{G2}, 8)$, where the ω_i diverged from 1/4 for very large i and no trustworthy $\bar\omega_m$ could be generated for large m, the new procedure did not improve the log log rates shown in Table 4 (observe that they already are very close to 1/2) and did not generate better rates for $i > 32$.

A natural question in blow-up problems is whether the development of singularities can be prevented by the addition of some suitable dissipative term in the equation. In the note [4] we tested with a similar numerical method the 'stability' of the blow-up and the blow-up rates of the singular radial solutions of the NLS in two and three dimensions, when the linear, zeroth-order damping term $-\delta u$, where δ is a small positive number, is added to the right-hand side of (1.2a). Our conclusion was that damping of small size does not prevent the formation of

singularities, even in the critical case, and that, predictably, the blow-up rates are close to their counterparts of the undamped equation. These computational results complement the theory of [47], which is valid in the three-dimensional case, and were subsequently verified in the systematic numerical and analytical treatment of the problem by Fibich, [17].

Another problem of major interest is to describe how non-radial solutions of the NLS blow up, say in two space dimensions. In [29] the cited dynamic rescaling techniques of the previous papers of that group were extended to the general case of the non-radially symmetric equation. It was demonstrated numerically in [29] that initial data with a single peak evolves into locally radially symmetric solutions that proceed to blow up, presumably at the critical radial case rates. In this direction, an adaptive finite element code capable of simulating $2-$D non-radially symmetric solutions has been recently developed, [25]. In particular, the code is capable of following multi-peak blow-up. This new code follows spatial and temporal mesh refinement strategies similar to those used in the present work. A more radical departure consists in the use of nonconforming elements in space following a formulation pioneered in [5] and subsequently extended in [6] and [24]. Experiments conducted so far show that several peaks may blow up simultaneously and confirm the results of [29] in that the peaks evolve into locally radially symmetric solutions.

The computational results reported in this paper and its companions, taken together with similar blow-up computations for the generalized Korteweg–de Vries equation (cf., e.g., [10]), indicate that suitably adaptive finite element techniques can describe accurately the development of point blow-up singularities of solutions of nonlinear dispersive wave equations. A very interesting but hard problem lies ahead: to understand how such adaptive mesh refinement mechanisms really work, and prove rigorously that they permit discrete solutions to blow up, provided the solution of the p.d.e. does.

Acknowledgements. The authors would like to thank Prof. G. Papanicolaou for many lectures and discussions on the blow-up of NLS and comments and suggestions on the material of this paper, and Prof. C. Sulem for her suggestion on computing the phase constant in the critical case. They also thank the referees for their suggestions and Mr. D. Mitsoudis for performing some of the rate computations in the revised version of the paper.

The research reported in this paper was materially aided by the Institute of Applied and Computational Mathematics of the Research Center of Crete, FO.R.T.H., the Science Alliance of the University of Tennessee, and a joint travel grant of the National Science Foundation, USA, and the General Secretariat of Research and Technology, Greece. To these institutions and agencies the authors express their gratitude.

References

1. G. D. Akrivis, V. A. Dougalis and O. A. Karakashian, *On fully discrete Galerkin methods of second-order temporal accuracy for the nonlinear Schrödinger equation,* Numer. Math. **59** (1991) 31–53.
2. G. Akrivis, V. A. Dougalis and O. A. Karakashian, *Solving the systems of equations arising in the discretization of some nonlinear p.d.e.'s by implicit Runge-Kutta methods,* Modél. Math. Anal. Numér. **31** (1997) 251–288.
3. G. D. Akrivis, V. A. Dougalis, O. A. Karakashian and W. R. McKinney, *Galerkin-finite element methods for the Nonlinear Schrödinger Equation,* in Advances on Computer Mathematics and its Applications, ed. by E. Lipitakis, pp. 85–106, World Scientific, Singapore 1993.
4. G. D. Akrivis, V. A. Dougalis, O. A. Karakashian and W. R. McKinney, *Numerical approximation of singular solutions of the damped Nonlinear Schrödinger Equation,* in ENUMATH 97, ed. by H. G. Bock *et al.*, pp. 117–124, World Scientific, Singapore 1998.
5. G. A. Baker, *Finite element methods for elliptic equations using nonconforming elements,* Math. Comp. **31** (1977) 45–59.

6. G. A. Baker, W. N. Jureidini and O. A. Karakashian, *Piecewise solenoidal vector fields and the Stokes problem,* SIAM J. Numer. Anal. **27** (1990) 1466–1485.
7. M. Berger and R. V. Kohn, *A rescaling algorithm for the numerical calculation of blowing-up solutions,* Comm. Pure Appl. Math. **41** (1988) 841–863.
8. A. L. Bertozzi, M. P. Brenner, T. F. Dupont, and L. P. Kadanoff, *Singularities and similarities in interface flows,* in Trends and Perspectives in Applied Mathematics, ed. by L. Sirovich, pp. 155–208, Springer–Verlag, New York 1994.
9. J. L. Bona, V. A. Dougalis, O. A. Karakashian, and W. R. McKinney, *Fully discrete methods with grid refinement for the generalized Korteweg–de Vries equation,* in Viscous Profiles and Numerical Methods for Shock Waves, ed. by M. Shearer, SIAM, Philadelphia 1991.
10. J. L. Bona, V. A. Dougalis, O. A. Karakashian, and W. R. McKinney, *Conservative, high-order numerical schemes for the generalized Korteweg–de Vries equation,* Phil. Trans. R. Soc. London A **351** (1995) 107–164.
11. C. J. Budd, S. Chen and R. D. Russell, *New self-similar solutions of the nonlinear Schrödinger equation with moving mesh computations,* J. Comp. Phys. **152** (1999) 756–789.
12. T. Cazenave, *Blow up and scattering in the nonlinear Schrödinger equation*, Textos de Métodos Matemáticos **30**, Instituto de Matématica, UFRJ, Rio de Janeiro 1994.
13. T. Cazenave and A. Haraux, *Introduction aux problèmes d'évolution semi-linéaires,* Mathématiques et Applications No 1, SMAI-Ellipses, Paris 1990.
14. R. Y. Chiao, E. Garmire and C. Townes, *Self-trapping of optical beams,* Phys. Rev. Lett. **73** (1964) 479–482.
15. T. F. Dupont, R. E. Goldstein, L. P. Kadanoff, and S.–M. Zhou, *Finite time singularity formation in Hele–Shaw systems,* Phys. Rev. E **47** (1993) 4182–4196.
16. G. Fibich, *Self-focusing in the nonlinear Schrödinger equation for ultrashort laser-tissue interactions,* Ph.D. Thesis, New York University, New York 1994.
17. G. Fibich, *Self-focusing in the damped nonlinear Schrödinger equation,* SIAM J. Appl. Math. **61** (2001) 1680–1705.
18. G. Fibich and G. Papanicolaou, *Self-focusing in the perturbed and unperturbed nonlinear Schrödinger equation in critical dimension,* SIAM J. Appl. Math. **60** (1999) 183–240.
19. G. M. Fraiman, *Asymptotic stability of manifold of self-similar solutions in self-focusing,* Soviet Physics JETP **61** (1985) 228–233.
20. J. Ginibre, *Introduction aux équations de Schrödinger non linéaires,* Paris Onze édition **L161**, Université de Paris–Sud, Orsay 1998.
21. J. Ginibre and G. Velo, *On a class of nonlinear Schrödinger equations I: the Cauchy problem, general case,* J. Funct. Anal. **32** (1979) 1–32.
22. R. T. Glassey, *On the blowing up of the solutions in the Cauchy problem for nonlinear Schrödinger equations,* J. Math. Phys. **18** (1977) 1974–1977.
23. O. Karakashian, G. D. Akrivis and V. A. Dougalis, *On optimal-order error estimates for the Nonlinear Schrödinger Equation,* SIAM J. Numer. Anal. **30** (1993) 377–400.
24. O. A. Karakashian and W. N. Jureidini, *A nonconforming finite element method for the stationary Navier-Stokes equations.* SIAM J. Numer. Anal. **35** (1998) 93–120.
25. O. A. Karakashian and M. Plexousakis, *Adaptive methods for nonradially symmetric solutions of the Nonlinear Schrödinger equation.* To appear.
26. T. Kato, *On nonlinear Schrödinger equations,* Annales Inst. H. Poincaré, Phys. Théor. **46** (1987) 113–129.
27. N. E. Kosmatov, V. F. Shvets and V. E. Zakharov, *Computer simulation of wave collapses in the nonlinear Schrödinger equation,* Physica D **52** (1991) 16–35.
28. M. J. Landman, G. C. Papanicolaou, C. Sulem and P. L. Sulem, *Rate of blowup for solutions of the nonlinear Schrödinger equation at critical dimensions,* Phys. Rev. A **38** (1988) 3837–3843.
29. M. J. Landman, G. C. Papanicolaou, C. Sulem, P. L. Sulem and X. P. Wang, *Stability of isotropic singularities for the nonlinear Schrödinger equation* Physica D **47** (1991) 393–415.
30. B. Le Mesurier, G. Papanicolaou, C. Sulem and P.-L. Sulem, *The focusing singularity of the nonlinear Schrödinger equation,* in Directions in Partial Differential Equations, M.G. Crandall, P.H. Rabinowitz and R.E. Turner, eds, pp. 159–201, Academic Press, New York 1987.
31. B. J. Le Mesurier, G. Papanicolaou, C. Sulem, and P. L. Sulem, *Focusing and multifocusing solutions of the nonlinear Schrödinger equation,* Physica D **31** (1988) 78–102.
32. B. J. Le Mesurier, G. Papanicolaou, C. Sulem and P. L. Sulem, *Local structure of the self-focusing singularity of the nonlinear Schrödinger equation,* Physica D **32** (1988) 210–226.
33. V. M. Malkin, *On the analytical theory for stationary self-focusing of radiation,* Physica D **64** (1993) 251–266.

34. D. W. McLaughlin, G. C. Papanicolaou, C. Sulem and P. L. Sulem, *Focusing singularity of the cubic Schrödinger equation,* Phys. Rev. A **34** (1986) 1200–1210.
35. F. Merle, *Blow up phenomena for critical nonlinear Schrödinger and Zakharov equations,* in the Proceedings of the International Congress of Mathematicians, Berlin 1998, Doc. Math. J. DMV **3** (1998) 57–66.
36. J. Rasmussen and K. Rypdal, *Blow-up in Nonlinear Schrödinger Equations, Parts I and II,* Physica Scripta **33** (1986) 481–504.
37. P. A. Robinson, *Nonlinear wave collapse and strong turbulence,* Rev. Mod. Phys. **69** (1997) 507–573.
38. M. J. Shelley, *A study of singularity formation in vortex–sheet motion by a spectrally accurate vortex method,* J. Fluid Mech. **244** (1992) 493–526.
39. A. I. Smirnov and G. M. Fraiman, *The interaction representation in the self-focusing theory,* Physica D **52** (1991) 2–15.
40. W. A. Strauss, *Nonlinear Wave Equations,* CBMS Regional Conference Series in Mathematics v. 73, AMS, Providence 1989.
41. C. Sulem and P.–L. Sulem, *Focusing Nonlinear Schrödinger equation and wave–packet collapse,* Nonlinear Analysis **30** (1997) 833–844.
42. C. Sulem and P.–L. Sulem, *The Nonlinear Schrödinger Equation,* Springer Verlag, New York 1999.
43. P.–L. Sulem, C. Sulem and A. Patera, *Numerical simulation of singular solutions to the two-dimensional cubic Schrödinger equation,* Comm. Pure Appl. Math. **37** (1984) 755–778.
44. V. I. Talanov, *Self-focusing of wave beams in nonlinear media,* JETP Lett. **2** (1965) 138–141.
45. Y. Tourigny and J. M. Sanz–Serna, *The numerical study of blow-up with application to a nonlinear Schrödinger equation,* J. Comp. Phys. **102** (1992) 407–416.
46. Y. Tourigny, J. M. Sanz–Serna and J. Ll. Morris, *Approximation of radial functions by piecewise polynomials on arbitrary grids,* Num. Methods for P.D.E.'s **7** (1991) 1–8.
47. M. Tsutsumi, *Nonexistence of global solutions to the Cauchy problem for the damped nonlinear Schrödinger equation,* SIAM J. Math. Anal. **15** (1984) 357–366.
48. S. N. Vlasov, L. V. Piskunova and V. I. Talanov, *Structure of the field near a singularity arising from self-focusing in a cubically nonlinear medium,* Soviet Physics JETP **48** (1978) 808–812.
49. M. I. Weinstein, *Nonlinear Schrödinger equation and sharp interpolation estimates,* Communs. in Math. Phys. **87** (1983) 567–576.
50. D. Wood, *The self-focusing singularity in the nonlinear Schrödinger equation,* Studies in Appl. Math. **71** (1984) 103–115.
51. V. E. Zakharov, *Collapse of Langmuir waves,* Soviet Physics JETP **35** (1972) 908–922.
52. V. E. Zakharov, S. L. Musher and A. M. Rubenchik, *Hamiltonian approach to the description of non-linear plasma phenomena,* Physics Reports **129** (1985) 286–366.
53. V. E. Zakharov and A. B. Shabat, *Exact theory of two–dimensional self–focusing and one–dimensional self–modulation of waves in nonlinear media,* Soviet Physics JETP **34** (1972) 62–69.
54. V. E. Zakharov and V. S. Synakh, *The nature of the self-focusing singularity,* Soviet Physics JETP **41** (1976) 465–468.

Computer Science Department, University of Ioannina, 451 10 Ioannina, Greece
E-mail address: akrivis@cs.uoi.gr

Mathematics Department, University of Athens, Panepistemiopolis, 157 84 Zographou, Greece, and Institute of Applied and Computational Mathematics, Research Center of Crete, FO.R.T.H., Greece.
E-mail address: doug@math.uoa.gr

Mathematics Department, University of Tennessee, Knoxville, Tennessee 37996, USA.
E-mail address: ohannes@math.utk.edu

Mathematics Department, North Carolina State University, Raleigh, N.C. 27695, USA.